20

Clustering Genes, Tissues, Cells and Bioactive Chemicals by Sphere SOM

Yuh Sugii[1], Takayuki Kudoh[1], Takayuki Otani[1], Masashi Ikeda[1],
Heizo Tokutaka[2] and Masaharu Seno[1]
[1]Okayama University,
[2]SOM JAPAN Inc.
Japan

1. Introduction

The technology of high throughput screening is nowadays widely available in life science especially in the fields of molecular diagnosis and drug discovery. This is due to the establishment of microarray procedure, which deals with huge number of genes at one time. Cluster analysis is usually performed on the results of DNA microarray experiments. However, the routine procedure of data mining dealing with the huge number of signal information obtained from microarray is not fixed yet. We can find various way of clustering in hierarchical and non-hierarchical methods, which are applied for the analyses. The most popular ones appear non-hierarchical clustering such as k-means (MacQueen, 1965), partitioning around medoids (Kaufman and Rousseeuw, 1990) and cluster affinity search technique (Ben-Dor et al., 1999).

We have employed spherical self organizing map (sSOM), which is also a non-hierarchical clustering, to cluster genes by gene expression profiles of cells and tissues (Tuoya et al., 2008). Analyzing various types of carcinoma cells and normal tissues, we could find interesting cell surface molecules, which should serve as the molecular markers. This procedure, which we are demonstrating, is rather new to the data analyses of gene clustering from the gene expression profiles obtained from DNA microarray technique. Flexible arrangement of the data obtained allows us to cluster cells and tissues as well as genes to find definitely fantastic direction of further advancement of study.

Furthermore, we applied sSOM to classify bioactive chemical compounds by their mechanism of action (MOA), which should enable us virtual screening in silico (Reddy et al., 2007). In recent years, many intriguing methods for virtual screening have been developed in this field (Gasteiger et al., 2003; Melville et al., 2009). Especially, ligand-based method is suitable for selecting drug candidates from enormous compounds library because it simply requires computational resources, which are less expensive. Although SOM has partly been used as a tool of ligand-based methods to classify compounds by their properties in chemoinformatics, spherical SOM has not been used in chemoinformatics to the best of our knowledge (Brüstle et al., 2002; Schneider & Nettekoven, 2003; Schneider & Schneider, 2003; Wang et al., 2005; Kaiser et al., 2007; Renner et al., 2007; Li & Gramatica, 2010). We propose here the extended application of sSOM to classify bioactive compounds by their MOA together with their structural information. In the future this procedure should

be extremely helpful in the field of drug discovery as well as those of molecular biology and oncology.
This chapter is dedicated to introduce our concept of the application of sSOM procedure.

2. Materials, methods and tools

2.1 Cell lines and cell culture

Human breast cancer derived cell lines Hs-578T, MCF-7, MDA-MB-134, MDA-MB-231, SK-BR-3, T-47D and ZR-75-1 were obtained from American Type Culture Collection (ATCC, VA). Hs-578T cells were cultured in DMEM containing 10 % fetal bovine serum (FBS), 10 μg/mL insulin and 2 mM L-glutamine. MCF-7 cells were cultured in MEM containing 10 % FBS, 10 μg/mL insulin and 2 mM L-glutamine. MDA-MB-134 cells were cultured in Leibovitz-15 containing 10 % FBS, 2 mM L-glutamine buffered with 10 mM HEPES. MDA-MB-231 cells were cultured in DMEM containing 10 % FBS and 2 mM L-glutamine. SK-BR-3 cells were cultured in RPMI 1640 containing 20 % FBS and 2 mM L-glutamine. T-47D cells cultured in RPMI 1640 containing 10 % FBS, 2 mM L-glutamine, 10 μg/mL insulin and 30 ng/mL EGF. ZR-75-1 cells were cultured in RPMI 1640 containing 10 % FBS. All cells were maintained at 37 ˚C in a humidified 5 % CO_2 atmosphere except MDA-MB-134 cells, which were maintained in 100 % air.

2.2 Preparation of total RNA and cDNA synthesis

Total RNA was extracted from the cells used in this study. Cells were harvested at a confluence of 80% for preparation using RNeasy Mini kits (Qiagen), following the manufacturer's instructions. Total RNA from human normal breast and mouse normal tissues was purchased from Stratagene (CA). RNA integrity and purity were assessed by $OD_{260/280}$ measurements and by the ratio of 28S and 18S rRNA with Experion system (BioRad Labs, VA). The total RNA was further treated with DNase and purified. The integrity of template RNA was assessed by $OD_{260/280}$ measurements. Twenty micrograms of total RNA was used to synthesize cDNA in the presence of aminoalkyl-dUTP. To monitor the efficiency of cDNA synthesis and hybridization control RNAs were added in the reaction as describe previously (Tuoya et al., 2008; Abou-Sharieha et al. 2009). Cy3-labeled cDNAs were prepared by indirect labeling method adapted from the Brown Web site (http://cmgm.stanford.edu/pbrown/protocols).

2.3 Microarray analysis

We originally proposed DNA microarray, which focused cell membrane-bound proteins to identify cell surface marker specific to the cells or tissues of interest (Tuoya et al., 2008; Abou-Sharieha et al. 2009). Two different microarrays were designed to contain 1,795 oligonucleotide probes corresponding to human genes and 1,405 corresponding to mouse genes, respectively. These genes were limited to those coding membrane-bound proteins so as to cover cell surface proteins. To avoid the effect of alternative splicing, the coding sequence for the membrane-bound region or GPI-anchor modified region was focused to design the oligonucleotide probes. The probes were conjugated on the slide glass coated with diamond-like carbon as described previously (Tuoya et al., 2005).
The Cy3-labeled cDNA synthesized above was hybridized to the cell surface marker DNA microarray in 5x SSC/0.5 % SDS solution at 55 °C for 15 h. After washing, arrays were scanned on a FLA8000 scanner (Fuji Film, Japan). Intensity for each spot of the array was

captured by GenePix® Pro5.1 image analysis software (Axon Instrument). The fluorescent intensity of each spot referred as ''relative fluorescent intensity (RFI)'', which represented the expression level of each gene. Gene expression levels were compared to one another by RFI value to identify differentially expressed genes.

2.4 Data filtering in breast cancer cell

In order to eliminate genes that did not change significantly between cancer cell lines and normal tissue, each gene was given a score S by a formula:

$$S = |N - C| - V_C$$

, where N, C and V_C denote the expression level of the gene in normal breast, the average of the expression levels of the gene in the seven cancer cell lines and the standard deviation of the gene expression level in the seven cancer cell lines, respectively. Genes were eliminated from further consideration when S<0 or S=0, since only the genes with a score greater than a threshold (i.e., zero) are deemed potentially significant (Tuoya et al., 2008).

2.5 sSOM analysis of gene expression

The expression levels of each gene were normalized among the breast cancer cell lines and normal breast tissue and among mouse normal tissues. First, the maximal RFI value of each gene was taken as 1, the minimum RFI was taken as 0 and other RFI values were linearly calculated into the values between 0 and 1. Secondly the average expression levels of each gene were calculated and each average was divided by the maximal average value. The resultant values were further multiplied to each normalized value calculated above. The normalized data were clustered and displayed by sSOM software Cluster Blossom (Ver. 1.0.2, SOM Japan Co-Ltd., http://www.somj.com/). The training of Cluster Blossom were performed 50 times. Other parameters were automatically set by the software. Then the dendrograms were drawn from the final map after training by group average method with a glyph value 1.0.

2.6 Datasets for chemicals

The dataset analyzed in this study was taken from the previous report, in which 131 compounds were classified by the self organizing map with screening data against the 60 human cancer cell lines as input vectors (van Osdol et al., 1994). All these compounds structure data were downloaded from NCI databases by using Enhanced NCI Database Browser (http://129.43.27.140/ncidb2/). The names of compounds analyzed in this study are listed in Table 2 with NSC Nos. and MOA.

2.7 Descriptors of chemicals

All downloaded structures were submitted to the chemical descriptor calculation software, CDK Descriptor Calculator GUI (ver. 1.0.5; http://rguha.net/code/java/cdkdesc.html) to calculate 283 theoretical descriptors, including molecular descriptors, bond descriptors and atom descriptors (Steinbeck et al., 2003).

2.8 Descriptor scaling and selection

All above calculated descriptors were normalized by each row that they have mean 0 and variance 1 by the function of "normalize" in the "som package" of statistical software R

(Windows Ver. 2.9.0; "Self-Organizing Map" R package Version 0.3-4, URL http://cran.r-project.org/; R Development Core Team, 2007, http://www.R-project.org/). All errors were deleted from this dataset and normalized dataset (116 compounds-by-215 descriptors matrix) was obtained.

2.9 sSOM analysis of chemicals

Clustering were performed with the software Cluster Blossom (Ver. 1.0.3, SOM Japan Co-Ltd.). The trained sSOM was developed using the dataset above mentioned as input vectors. The same training parameters of Cluster Blossom were used as described above. Similarly, the dendrogram was drawn from the trained map as described above. The accuracy of clustering A was calculated as following.

$$A = Nt_{Gi} / N_{Gi} \times 100$$

where Nt_{Gi} is the number of compounds correctly assigned in cluster Gi and N_{Gi} is the number of compounds assigned in cluster Gi where i depicts the number of cluster.

3. Results and discussion

3.1 sSOM clustering of human breast cancer cell lines

We performed DNA microarray gene expression analysis in order to screen genes commonly and specifically expressed in the seven cell lines derived from breast cancer when compared to normal breast. As the result of data filtering, 840 genes were found to suffice the criteria described in "2.4 Data filtering in breast cancer cell". The expression levels of these genes were then normalized and clustered by sSOM. The gene expression profiles were visualized on the sphere surface map and the dendrogram indicating themselves classified by the origin of the cells (Fig. 1). It is interesting to note that Hs-578T and MDA-MB-231 cells, which are derived from basal-like breast cancer known to have poor prognosis, are clustered in the same group (Ray et al., 2010). T-47D, ZR-75-1, MCF-7 and MDA-MB-134 cells, which are derived from luminal breast cancer, are well known to have good prognosis. Since SK-BR-3 cells are Her2 positive, which is an efficient target for the cancer therapy, and derived from breast cancer of medium level of prognosis. Thus, the gene expression profiles were successfully visualized by the sSOM clustering, suggesting the clusters of prognosis. From the patterns, cells derived from luminal breast cancer appear to be clustered into three groups of "close to normal", "medium" and "poorer". Namely, it might be possible to diagnose SK-BR-3 cells as "close to normal" while MDA-MB-134 as poorer than the other luminal derived cells.

In order to find genes highly expressed in all the seven cancer cell lines, sSOM was performed with an assumptive gene inserted into the dataset of the 840 genes. The assumptive gene stood for an ideal point IP, which was supposed to be expressed in all the breast cancer cell lines analyzed in this study but not in the normal breast tissue, so that the genes clustered close to IP should be potential diagnostic markers of breast cancer. In the result of sSOM clustering, IP was mapped in the red part of the pattern in all the seven cancer cell lines (Fig. 1) but blue in normal breast tissue. Since this mapped position of IP is consistent with the assumption, the genes close to IP should be selected as candidates of cancer-specific genes on the sSOM. Each spot on the surface of sSOM contains a group of clustered genes (Fig. 2). The spots mapped close to IP are shown in Fig. 2 and the candidate genes clustered in each spot are listed in Table 1. It is noteworthy that ErbB3 and ROBO2 have been nominated as potential diagnostic

markers here and some reports are found describing their relationships with breast cancers (Lemoine et al., 1992; Gasparini, 1994; Quinn et al. 1994 Travis et al., 1996; Naidu et al., 1998; Fogel et al., 1999; Holbro et al., 2003; Barnes et al., 2005; Schabath et al., 2006; Shiau et al. 2008). MUC1 is also known as a diagnostic marker in various cancers including breast cancers (Singh et al., 2008). Considering the results that contain these potential candidates, the other genes listed in Table 1 could be a potential candidate for the diagnostic marker of breast cancers still unknown.

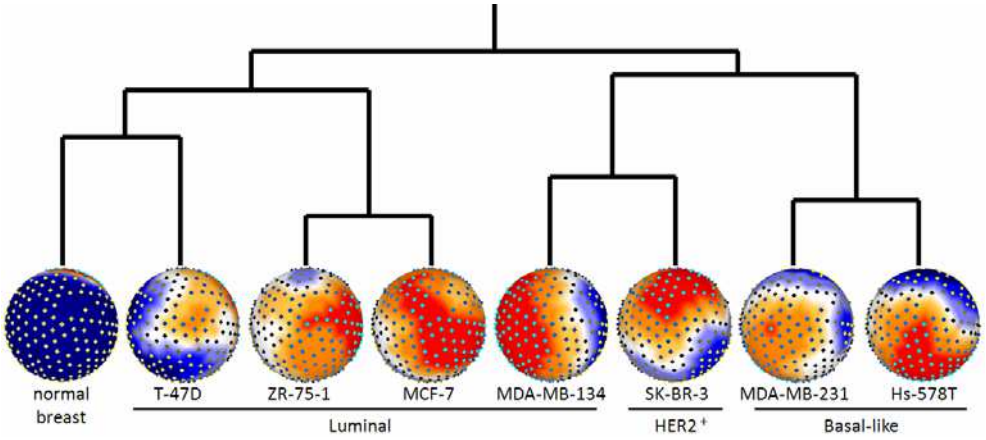

Fig. 1. The gene expression profiles analyzed by sSOM for cancer derived cell lines and normal breast. The normalized data set was clustered and visualized by Cluster Blossom. Each position of genes is fixed on the global surface. The colors indicate the expression level for each gene. Red, high; yellow, slightly high; white, median; light blue, slightly low; deep blue, low. See text for the names of cell lines and diagnostic levels. The alignment of cells is the result of sSOM clustering, which was drawn by dendrogram

Gene No.	GenBank Accession No.	Gene Name
1586	NM_032038	spinster-like protein
1423	NM_016372	seven transmembrane domain orphan receptor
1784	AH006947	vitelliform macular dystrophy protein 2
1777	M29366	v-erb-b2 erythroblastic leukemia viral oncogene homolog 3 (ErbB3)
1682	NM_012471	transient receptor potential cation channel, subfamily C, member 5
734	NM_002099	glycophorin A (includes MN blood group)
1399	AF040991	roundabout, axon guidance receptor, homolog 2 (ROBO2)
163	NM_001188	BCL2-antagonist/killer 1
247	NM_001218	carbonic anhydrase XII
1699	NM_003271	transmembrane 4 superfamily member 7
241	NM_022131	calsyntenin 2
1015	NM_002456	mucin 1, transmembrane (MUC1)

Table 1. Candidate genes for the potential diagnostic marker for breast cancer as picked up from genes commonly expressed in all the cancer derived cells studied in this paper

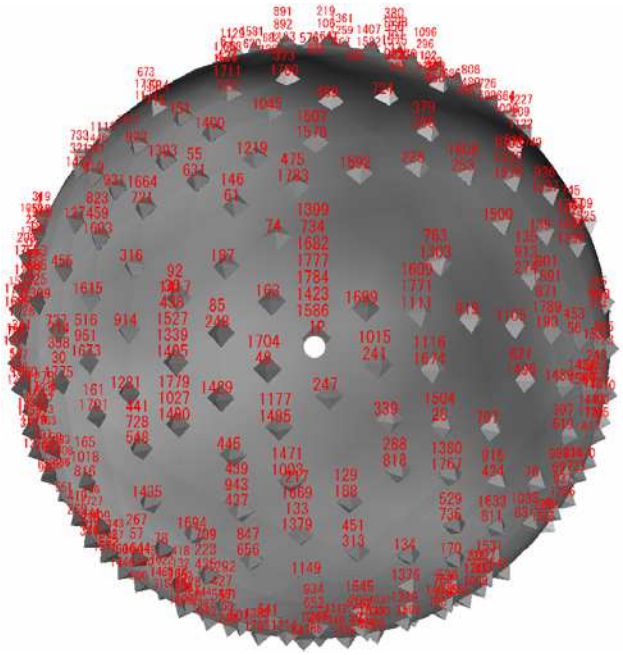

Fig. 2. The locations of ideal point IP (white spot) clustered by sSOM. This global surface is the same with those in Fig. 1 without colors. Each gray spot on the surface of sSOM contains a group of clustered genes, which were depicted with the gene numbers in red. The genes clustered close to IP are summarized in Table 1

3.2 sSOM clustering of mouse normal tissues

In this section, gene expression profiles of normal tissues in mouse were clustered by sSOM. Since the breast cancer cell lines were successfully clustered, we expected normal tissues should be also clustered with the features of each tissue. Clustering of brain, colon, heart, kidney, liver, lung, muscle, small intestine, spleen, stomach, testis and thymus was performed and the resultant gene expression profiles were aligned on the anatomical sketch of mouse body (Fig. 3). The relationship between each tissue was shown in a global map obtained by sSOM (Fig. 4). In this map, each distance between the nodes was not adjusted to a sphere surface (glyph =0) but reflected the distance when calculated by SOM (glyph =1.0) resulting in a meteoritic form of map.

The alignment of gene expression profiles around the body sketch reveals some similarities between the tissues. The similarity of the profiles between colon and intestine appears consistent. The similarity of profiles between spleen and thymus also sounds reasonable because of the deep relationship of these tissues with immunological system. The similarity is also found in heart, liver and lung. Although it is difficult to explain their close relationship from the embryonic development of tissues in mouse, it might be important to try to make viewpoints shared in these three tissues but not in other tissues as suggested by the sSOM clustering. Further application of sSOM on the gene expression profiles comparing with normal tissues and diseased tissues would lead to a challenging opportunity to find novel diagnostic markers in the future.

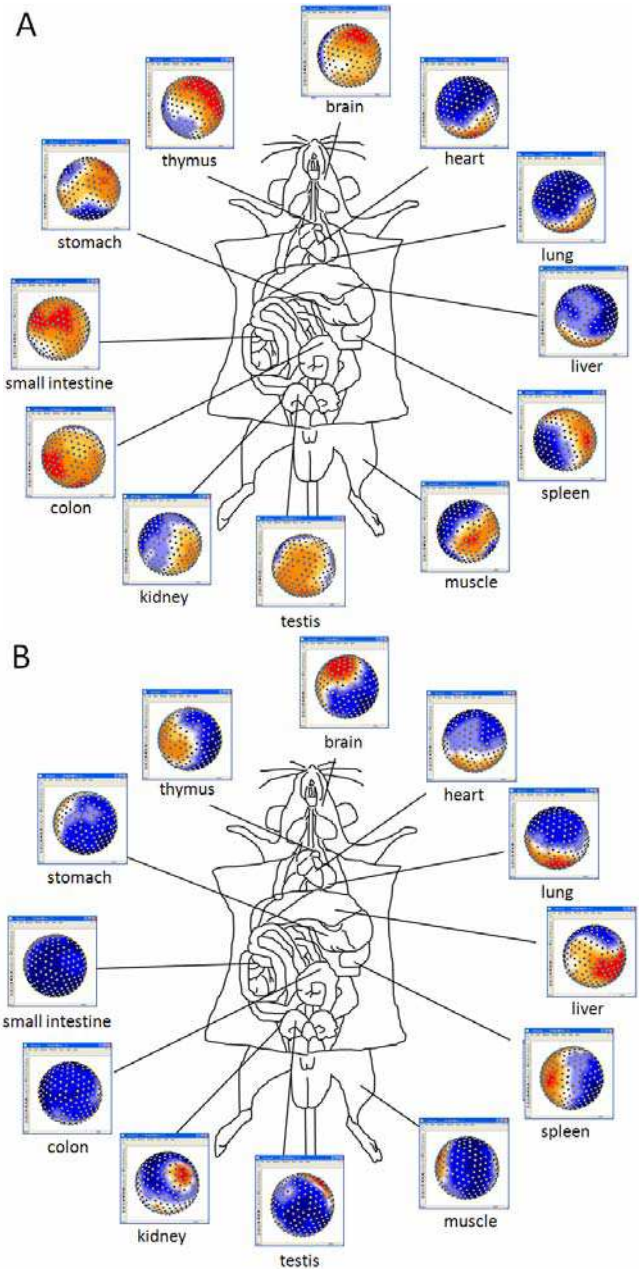

Fig. 3. Gene expression profiles of mouse normal tissues clustered by sSOM. The normalized data set was clustered and visualized by Cluster Blossom. Each position of genes is fixed on the global surface. See Fig. 1 for the colors indicating the expression level for each gene. Views of clustered global map from front side (A) and back side (B)

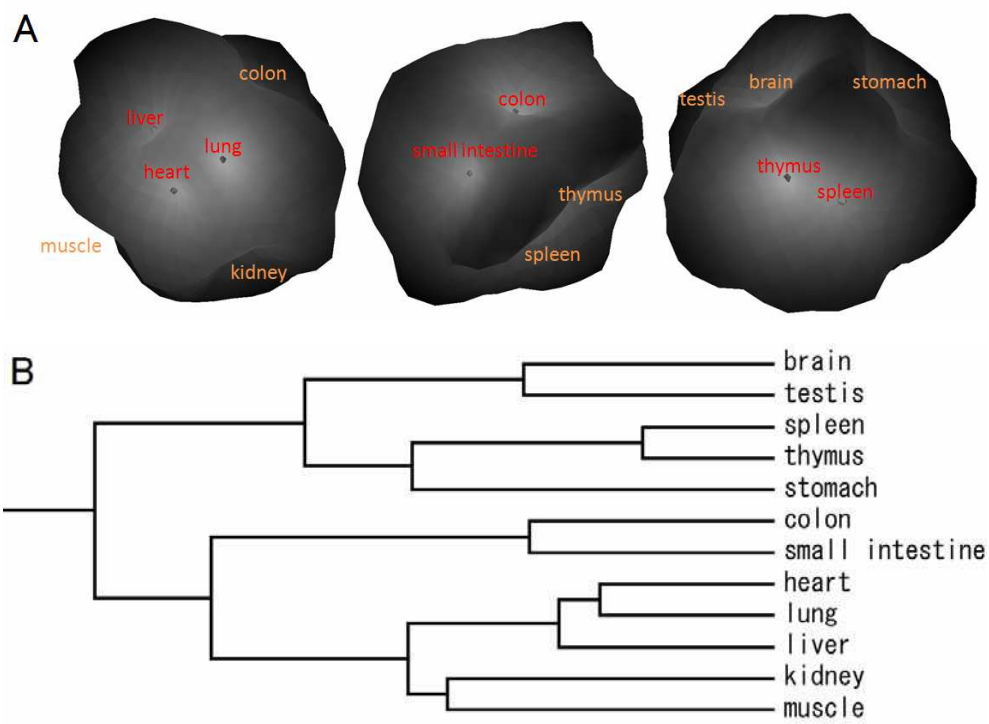

Fig. 4. Meteoritic map clustering normal mouse tissues (A) and dendrogram of clustered normal mouse tissues (B). Each distance between the nodes were calculated with glyph value 1.0. (A) Views from three different sides of the map. Tissues depicted in red letters are on the front side and those in orange letters are on the other side. The farther the relationship between the tissues, the darker the shadow is. (B) Dendrogram was calculated from the results of clustering by sSOM

3.3 sSOM clustering of bioactive chemicals

The bioactive compounds previously screened for anti-cancer reagents were evaluated for clustering in this study. The compounds were clustered by sSOM. The dendrogram was drawn based on the trained map by group average method to obtain 9 clusters of compounds, which were colored by their clusters on the surface of global map (Fig. 5). The compounds in the dataset are summarized in Table 2 with their assigned MOA and the cluster groups.

Table 3 shows the clustering results of compounds. The accuracy of clustering was overall 86.2%, ranging from 60 to 100% in each cluster. The alkylating agents, AC, A7, and AI, are misclassified relatively in higher frequency than other agents. It is interesting to note the anti-DNA agents, DI, DP, and DR, and the inhibitors of nucleotide synthesis, RI, RO, and R, are clustered into the same group. This might be the result due to the character of these agents associating with the enzymes associated with nucleotide metabolisms.

In this study, 16 compounds (ID 5, 17, 29, 33, 44, 46, 52, 64, 81, 86, 88, 92, 93, 96, 99) were misclassified. These results suggest that they might have another activity other than those experimentally defined because small organic compounds frequently exhibit

polypharmacology. In fact, trimetrexate (ID 88) and DUP785 (ID 96) might have topoisomerase inhibiting activity because both of them have resemble planar heteroaromatic ring, which is the feature of topoisomerase inhibitor. Additionally, mitzolamide (ID 89) has also heteroaromatic ring implying DNA interacting ability. The chemical structures of these three compounds are shown in Fig. 6. Currently, exploring new targets and activity of already approved drugs is fascinating strategy to develop novel therapeutic drugs with less risks of the clinical trial (Keiser et al., 2009). Although further investigation is needed, sSOM would be a comprehensive and useful tool to classify the compounds and to find novel activities in themselves.

ID	NSC No.	Drug Name	MOA	cluster
1	NSC740	Methotrexate	RF	G1
2	NSC750	Busulfan	A7	G6
3	NSC752	Thioguanine	DI	G7
4	NSC755	Thiopurine	DI	G7
5	NSC757	Colchicine	TU	G9
6	NSC762	Mechlorethamine	A7	G6
7	NSC1895	Guanazole	DR	G7
8	NSC3088	Chlorambucil	A7	G6
9	NSC6396	Thiotepa	A7	G7
10	NSC8806	Melphalan	A7	G6
11	NSC9706	Triethylenemelamine	A7	G7
12	NSC19893	Fluprouracil	R	G7
13	NSC25154	Pipobroman	A7	G6
14	NSC26980	Mitomycin	A2	G7
15	NSC27640	Floxuridine	DP	G7
16	NSC32065	Hydroxyurea	DR	G7
17	NSC33410	Colchicine derivative	TU	G9
18	NSC34462	Uracil mustard	A7	G6
19	NSC49842	Vinblastine sulfate	TU	G3
20	NSC51143	Pyrazoloimidazole	DR	G7
21	NSC56410	Porfiromycin	A2	G7
22	NSC63878	Cytarabine	DP	G7
23	NSC67574	Vincristine sulfate	TU	G3
24	NSC71261	beta-2'-Deoxythioguanosine	DI	G7
25	NSC71851	alpha-2'-Deoxythioguanosine	DI	G7
26	NSC73754	Fluorodopan	A7	G6
27	NSC79037	Lomustine	AC	G6
28	NSC82151	Daunorubicin	T2	G2

29	NSC83265	Trityl cysteine	TU	G9
30	NSC94600	Camptothecin	T1	G9
31	NSC95382	Camptothecin derivative	T1	G9
32	NSC95441	Semustine	AC	G6
33	NSC95466	PCNU	AC	G7
34	NSC95678	3-Hydroxypicolinealdehyde thiosemicarbazone	DR	G7
35	NSC100880	Camptothecin derivative	T1	G9
36	NSC102627	Yoshi-864	A7	G6
37	NSC102816	Azacytidine	RO	G7
38	NSC107124	Camptothecin derivative	T1	G9
39	NSC107392	5-Hydroxypicolinaldehyde thiosemicarbazone	DR	G7
40	NSC118994	Inosine glycodialdehyde	DR	G7
41	NSC122819	Teniposide	T2	G2
42	NSC123127	Doxorubicin	T2	G2
43	NSC125973	Paclitaxel derivative	TU	G3
44	NSC126771	Dichloroallyl lawsone	RO	G6
45	NSC127716	5-Aza-2'-deoxycytidine	DI	G7
46	NSC132313	Dianhydrogalactitol	A7	G7
47	NSC132483	Aminopterin	RF	G1
48	NSC134033	Aminopterine derivative	RF	G1
49	NSC135758	piperazinedione	A7	G6
50	NSC139105	Baker's soluble antifolate	RF	G5
51	NSC141540	Etoposide	T2	G2
52	NSC142982	Hycanthone	AI	G9
53	NSC143095	Pyrazofurin	RO	G7
54	NSC145668	Cyclocytidine	DP	G7
55	NSC14895	Ftorafur	R	G7
56	NSC153353	L-Alanosine	RO	G7
57	NSC153858	Maytansine	TU	G5
58	NSC163501	Acivicin	RI	G7
59	NSC164011	Zorubicin	T2	G2
60	NSC167780	Asaley	A7	G5
61	NSC172112	Spiromustine	A7	G6
62	NSC174121	Methotrexate derivative	RF	G1
63	NSC176323	Camptothecin derivative	T1	G9
64	NSC178248	Chlorozotocin	AC	G7

65	NSC182986	Diaziridinylbenzoquinone	A7	G7
66	NSC184692	Aminopterin derivative	RF	G1
67	NSC224131	N-(phosphonoacetyl-L-aspartic acid, tetrasodium salt)	RO	G7
68	NSC249910	Camptothecin derivative	T1	G9
69	NSC249992	Amsacrine	T2	G9
70	NSC264880	5,6-Dihydro-5-azacytidine	RO	G7
71	NSC267469	Deoxydoxorubicin	T2	G2
72	NSC268242	N,N-Dibenzyl daunomycin	T2	G2
73	NSC269148	Menogaril	T2	G2
74	NSC295500	Camptothecin derivative	T1	G9
75	NSC295501	Camptothecin derivative	T1	G9
76	NSC296934	Teroxirone	A7	G7
77	NSC301739	Mitoxantrone	T2	G2
78	NSC303812	Aphidicolin glycinate	DP	G4
79	NSC308847	Amonafide	T2	G9
80	NSC329680	Hepsulfam	A7	G6
81	NSC330500	Geldanamycin	DP	G9
82	NSC332598	Rhizoxin	TU	G5
83	NSC337766	Bisantrene	T2	G9
84	NSC338947	Clomesone	AC	G6
85	NSC344007	Piperazine alkylator	A7	G6
86	NSC348948	Cyclodisone	AC	G7
87	NSC349174	Oxanthrazole	T2	G2
88	NSC352122	Trimetrexate	RF	G9
89	NSC353451	Mitozolamide	AC	G7
90	NSC354646	Morpholino adriamycin	T2	G2
91	NSC355644	Anthrapyrazole derivative	T2	G2
92	NSC357704	Cyanomorpholinodoxorubicin	AI	G2
93	NSC361792	Thiocolchicine	TU	G9
94	NSC364830	Camptothecin derivative	T1	G9
95	NSC366140	Pyrazoloacridine	T2	G9
96	NSC368390	DUP785 (brequinar)	RO	G9
97	NSC374028	Camptothecin derivative	T1	G9
98	NSC376128	Dolastatin 10	TU	G5
99	NSC406042	Allocolchicine	TU	G9
100	NSC409962	Carmustine	AC	G6

101	NSC603071	Camptothecin derivative	T1	G9
102	NSC606172	Camptothecin derivative	T1	G9
103	NSC606173	Camptothecin derivative	T1	G9
104	NSC606497	Camptothecin derivative	T1	G9
105	NSC606499	Camptothecin derivative	T1	G9
106	NSC606985	Camptothecin derivative	T1	G9
107	NSC608832	Paclitaxel derivative	TU	G3
108	NSC610456	Camptothecin derivative	T1	G9
109	NSC610457	Camptothecin derivative	T1	G9
110	NSC610458	Camptothecin derivative	T1	G9
111	NSC610459	Camptothecin derivative	T1	G9
112	NSC618939	Camptothecin derivative	T1	G9
113	NSC623017	an. Antifol II	RF	G1
114	NSC629971	Camptothecin derivative	T1	G9
115	NSC633713	an. Antifol II	RF	G1
116	NSC643833	Camptothecin derivative	T1	G9

Table 2. Compounds in the dataset and the result of clustering. Abbreviations in MOA are as following. DNA alkylating agents: A2, alkylating at N-2 position of guanine; AC, alkyl transferase-dependent cross-linkers; A7, alkylating at N-7 position of guanine; AI, DNA intercalators. Anti-DNA agents: DI, incorporated; DP, polymerase inhibitors; DR, ribonuclease reductase inhibitors. Nucleotide synthesis inhibitors: RF, antifolates; RI, irreversible inhibitors; RO, anti other precursors; R, unknown locus of inhibition. Topoisomerase inhibitor: T1, topoisomerase I inhibitors; T2, topoisomerase II inhibitors. Tubulin-active antimitotic agents: TU

cluster group	map color	MOA	Accuracy (%)
G1	blue	RF	100
G2	yellow	T2	92
G3	gray	TU	100
G4	green	DP	100
G5	pink	TU	60
G6	cyan	AC, A7	94
G7	yellowish green	DI, DP, DR, RI, RO, R	82
G8	white	A2, A7	100
G9	red	T1, T2	75

Table 3. Summary of clustering compounds in this study. See Table 2 for the abbreviations for MOA. Accuracy was calculated as described in “2.9 sSOM analysis of Chemicals“

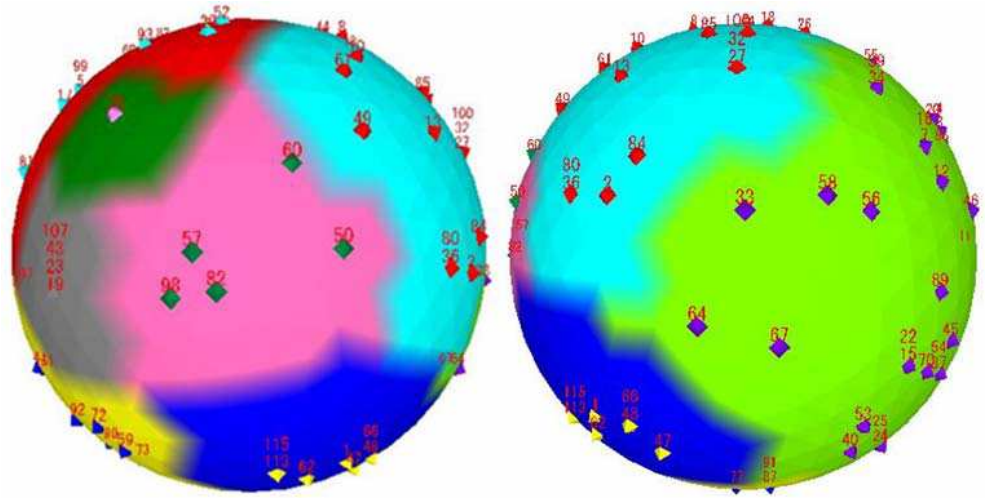

Fig. 5. Projections of clustered bioactive compounds by sSOM. Cluster colors: G1, blue; G2, yellow; G3, gray; G4, green; G5, pink; G6, cyan; G7, yellowish green; G8, white; G9, red. Numbers at the nodes indicate the ID of compounds. Two views on a single global map are shown from the opposite directions

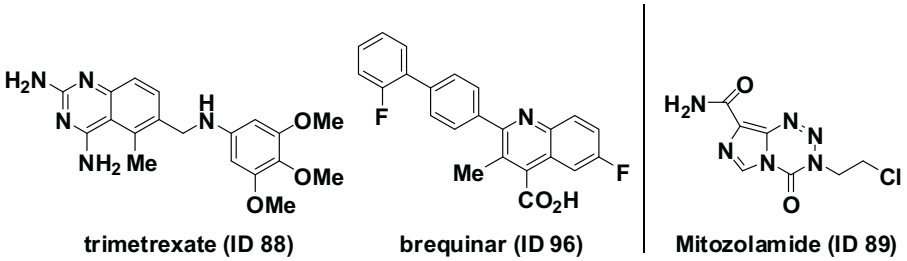

Fig. 6. Chemical structures of trimetrexate (ID 88), DUP 785 (ID 96), and mitozolamide (ID 89)

4. Conclusions

In order to characterize cells and tissues, gene expression profiling is one of the most popular procedures nowadays. Through these procedures, identification of cell surface markers specific to some cells or tissues is a key for diagnosing and molecular targeting. DNA microarray is a high-throughput technology believed to be a powerful tool to find genes differentially expressed in the cells or tissues. Although it can provide critically important and useful information even from one experiment, the amount of data is usually too large to be handled. Therefore, highly sophisticated software is expected to support to transform the multidimensional datasets into simple dimensions or glyphs. For example, visual cues such as shape and color, which make it comprehensive for researchers to

recognize and analyze the patterns hidden in the datasets. Here we successfully demonstrated cell surface marker analyses using our DNA microarray coupled with novel sSOM clustering procedure. The cell surface markers, which are common and specific to cancer derived cells, are proposed in this study and further assessment is now underway.
Here we have also examined sSOM for the classification of chemical compounds. sSOM successfully clustered 116 anti-cancer agents into 9 groups by their MOA using simple chemical descriptors as inputs. So we are now trying to apply this procedure to larger dataset for virtual screening.
Thus, we conclude sSOM is a powerful tool for data mining, knowledge discovery and visualization of multi-dimensional data.

5. References

Abou-Sharieha, S; Sugii, Y; Tuoya; Yu, D; Chen, L; Tokutaka, H & Seno, M. (2009) Identifi cation of TM9SF2 as a candidate of the cell surface marker common to breast carcinoma cells. *Clin. Oncol. Cancer Res.* 6(1), 1-9, ISSN: 1674-5361.

Barnes, N.L.; Khavari, S.; Boland, G.P.; Cramer, A.; Knox, W.F. & Bundred, N.J. (2005) Absence of HER4 expression predicts recurrence of ductal carcinoma in situ of the breast. *Clin. Cancer Res*. 11(6), 2163-2168, ISSN: 1078-0432.

Ben-Dor, A.; Shamir, R. & Yahkini, Z. (1999) Clustering gene expression patterns. *Journal of Computational Biology*, 6(3/4) 281-297, ISSN: 1557-8666.

Brüstle, M.; Beck, B.; Schindler, T.; King, W.; Mitchell, T & Clark T. (2002) Descriptors, physical properties, and drug-likeness. *J. Med. Chem.* 45(16), 3345-3355, ISSN: 0022-2623.

Fogel, M.; Friederichs, J.; Zeller,Y.; Husar, M.;, Smirnov, A.; Roitman, L.; Altevogt, P. & Sthoeger, Z.M. (1999) CD24 is a marker for human breast carcinoma. *Cancer Lett*. 143(1), 87-94, ISSN: 0304-3835.

Gasparini, G.; Gullick, W.J.; Maluta, S.; Dalla Palma, P.; Caffo, O.; Leonardi, E.; Boracchi, P.; Pozza, F.; Lemoine, N.R.; & Bevilacqua, P. (1994) C-erbB-3 and c-erbB-2 protein expression in node-negative breast carcinoma-an immunocytochemical study. *Eur J Cancer*, 30A(1), 16-22, ISSN: 0014-2964.

Gasteiger, J.; Teckentrup, A.; Terfloth, L. & Spycher, S. (2003) Neural networks as data mining tools in drug design. *J. Phys. Org. Chem.* 16 (4), 232-245, ISSN: 1099-1395.

Holbro, T.; Civenni, G.; Hynes, N.E. (2003) The ErbB receptors and their role in cancer progression. *Exp Cell Res.* 284(1), 99-110, ISSN: 0014-4827.

Kaiser, D.; Terfloth, L.; Kopp, S.; Schulz, J.; Laet, de R.; Chiba, P.; Ecker F. G. & Gasteiger J. (2007) Self-organizing maps for identification of new inhibitors of P-glycoprotein. *J. Med. Chem.* 50(7), 1698-1702, ISSN: 0022-2623.

Kaufman, L. & Rousseeuw, P.J. (1990) Finding Groups in Data: An Introduction to Cluster Analysis. John Wiley & Sons, ISBN: 978-0-471-73578-6, New York.

Keiser, M.J.; Setola, V.; Irwin, J.J.; Laggner, C.; Abbas, A.I.; Hufeisen, S.J.; Jensen, N.H.; Kuijer, M.B.; Matos, R.C.; Tran, T.B.; Whaley, R.; Glennon, R.A.; Hert, J.; Thomas, K.L.; Edwards, D.D.; Shoichet, B.K. & Roth, B.L. (2009) Predicting new molecular targets for known drugs. *Nature* 462(7270), 175-181, ISSN 0028-0836.

Lemoine, N.R.; Barnes, D.M.; Hollywood, D.P.; Hughes, C.M.;Smith, P.; Dublin, E.; Prigent, S.A.; Gullick, W.J.;& Hurst HC. (1992) Expression of the ERBB3 gene product in breast cancer. *Br J Cancer* 66(6), 1116-1121, ISSN 0007-0920.

Li J. & Gramatica P. (2010) Classification and virtual screening of androgen receptor antagonists. *J. Chem. Inf. Model.* 50(5), 861-874, ISSN: 1549-9596.

MacQueen, J. (1965) Some methods for classification and analysis of multivariate observations. In: *Proceedings of the 5th Berkeley Symposium on Mathematical Statistics and Probability*, pages 281-297.

Melville, J. L.; Burke, E. K.; & Hirst, J. D. (2009) Machine learning in virtual screening. *Combinatorial Chemistry and High Throughput Screening*, 12(4), 332-343, ISSN 1386-2073.

Naidu, R.; Yadav, M.; Nair, S. & Kutty, M.K.(1998) Expression of c-erbB3 protein in primary breast carcinomas. *Br J Cancer.* 78(10), 1385-1390, ISSN 0007-0920.

Quinn, C.M.; Ostrowski, J.L.; Lane, S.A.; Loney, D.P.; Teasdale, J., Benson, F.A. (1994) C-erbB-3 protein expression in human breast cancer: comparison with other tumor variables and survival. *Histopathology*, 25(3), 247-252, ISSN 0309-0167.

R Development Core Team (2007) R: A language and environment for statistical computing. R Foundation for Statistical Computing, Vienna, Austria, ISBN 3-900051-07-0.

Ray, P.S.; Wang, J.; Qu, Y.; Sim, M.S., Shamonki, J; Bagaria, S.P.; Ye, X.; Liu, B.; Elashoff, D.; Hoon, D.S.; Walter, M.A.; Martens, J.W.; Richardson, A.L.; Giuliano, A.E.& Cui, X. (2010) FOXC1 is a potential prognostic biomarker with functional significance in basal-like breast cancer. *Cancer Res.*, 70(10), 3870-3786, ISSN 0008-5472.

Reddy S. A.; Pati P. S.; Kumar P. P.; Pradeep N. H. & Sastry N. G. (2007) Virtual screening in drug discovery – a computational perspective. *Current Protein And Peptide Science*, 8(4), 329-351, ISSN 1389-2037.

Renner, S.; Hechenberger, M.; Noeske, T.; Böcker, A.; Jatzke, C.; Schmuker, M.; Parsons, G. C.; Wel, T. & Schneider G. (2007) Searching for Drug Scaffolds with 3D Pharmacophores and Neural Network Ensembles. *Angew. Chem. Int. Ed.* 46(28), 5336-5339, ISSN: 1521-3773.

Schabath, H.; Runz, S.; Joumaa, S. & Altevogt, P. (2006) CD24 affects CXCR4 function in pre-B lymphocytes and breast carcinoma cells. *J Cell Sci.*, 119(Pt2), 314-325, ISSN: 0021-9533.

Schneider, G. & Nettekoven, M. (2003) Ligand-Based Combinatorial Design of Selective Purinergic Receptor (A_{2A}) Antagonists Using Self-Organizing Maps. *J. Comb. Chem.* 5(3), 233-237, ISSN: 1520-4766.

Schneider, P. & Schneider, G. (2003) Collection of Bioactive Reference Compounds for Focsed Library Design. *QSAR Comb. Sci.* 22(7), 713-718, ISSN: 1868-1751.

Shiau, C.E.; Lwigale, P.Y.; Das, R.M.; Wilson, S.A.& Bronner-Fraser M. (2008) Robo2-Slit1 dependent cell-cell interactions mediate assembly of the trigeminal ganglion. *Nat. Neurosci.*, 11(3), 269-276, ISSN: 1097-6256.

Singh, A.P.; Senapati, S.; Ponnusamy, M.P.;, Jain, M.; Lele, S.M.; Davis, J.S.; Remmenga, S.& Batra SK. (2008) Clinical potential of mucins in diagnosis, prognosis, and therapy of ovarian cancer. *Lancet Oncol.* 9(11), 1076-1085, ISSN: 1470-2045.

Steinbeck, C.; Han, Y.; Kuhn, S.; Horlacher, O.; Luttmann, E. & Willighagen, E. (2003) The chemistry development kit (CDK): An open source Java library for chemo- and bioinformatics. *J. Chem. Inf. Comput. Sci.* 43(2), 493-500, ISSN: 1549-9596.

Travis, A.; Pinder, S.E.; Robertson, J.F.; Bell, J.A.; Wencyk, P.; Gullick, W.J.; Nicholson, R.I.; Poller, D.N.; Blamey, R.W.; Elston, C.W. & Ellis, I.O. (1996) C-erbB-3 in human breast carcinoma: expression and relation to prognosis and established prognostic indicators. *Br J Cancer* 74(2), 229-233, ISSN 0007-0920.

Tuoya; Hirayama, K; Nagaoka, T; Yu, D; Fukuda, T; Tada, H; Yamada, H. & Seno M. (2005) Identification of cell surface marker candidates on SV-T2 cells using DNA microarray on DLC-coated glass. *Biochem. Biophys. Res. Commun.* 334(1), 263-268, ISSN: 0006-291X.

Tuoya; Sugii, Y.; Satoh, H.; Yu, D.; Matsuura, Y.; Tokutaka, H. & Seno, M. (2008) Spherical self-organizing map as a helpful tool to identify category-specific cell surface markers. *Biochem Biophys Res Commun.* 376(2), 414-418, ISSN: 0006-291X.

van Osdol, W.W.; Myers, T.G.; Paull, K.D.; Kohn, K.W. & Weinstein, J.N. (1994) Use of the Kohonen self-organizing map to study the mechanisms of action of chemotherapeutic agents. *J. Natl Cancer Inst.* 86(24), 1853-1859, ISSN 0027-8874.

Wang, Y.; Li, Y.; Yang, S. & Yang, L. (2005) Classification of substrates and inhibitors of P-glycoprotein using unsupervised machine learning approach. *J. Chem. Inf. Model.* 45(3), 750-757, ISSN: 1549-9596.

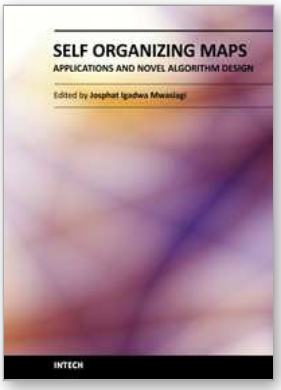

Self Organizing Maps - Applications and Novel Algorithm Design
Edited by Dr Josphat Igadwa Mwasiagi

ISBN 978-953-307-546-4
Hard cover, 702 pages
Publisher InTech
Published online 21, January, 2011
Published in print edition January, 2011

Kohonen Self Organizing Maps (SOM) has found application in practical all fields, especially those which tend to handle high dimensional data. SOM can be used for the clustering of genes in the medical field, the study of multi-media and web based contents and in the transportation industry, just to name a few. Apart from the aforementioned areas this book also covers the study of complex data found in meteorological and remotely sensed images acquired using satellite sensing. Data management and envelopment analysis has also been covered. The application of SOM in mechanical and manufacturing engineering forms another important area of this book. The final section of this book, addresses the design and application of novel variants of SOM algorithms.

InTech Europe
University Campus STeP Ri
Slavka Krautzeka 83/A
51000 Rijeka, Croatia
Phone: +385 (51) 770 447
Fax: +385 (51) 686 166
www.intechopen.com

InTech China
Unit 405, Office Block, Hotel Equatorial Shanghai
No.65, Yan An Road (West), Shanghai, 200040, China
中国上海市延安西路65号上海国际贵都大饭店办公楼405单元
Phone: +86-21-62489820
Fax: +86-21-62489821